Performance improvement of IPM motors by change of rotor shapes-application to electric vehicles

Bui Duc Hung*, Bui Minh Dinh, Dang Quoc Vuong

School of Electrical and Electronic Engineering, Hanoi University of Science and Technology.
*Corresponding author: hung.buiduc@hust.edu.vn
Received 27 Sep 2022; Revised 11 Oct 2022; Accepted 24 Oct 2022; Published 18 Nov 2022.
DOI: https://doi.org/10.54939/1859-1043.j.mst.83.2022.1-10

ABSTRACT

This paper has investigated the IPM motor from the Tesla rear-drive motor, with the single drive system delivers of 200 kW-450 Nm. This research concentrates on analyzing and evaluating the performances of the electric motor. Both the public data and improved simulation have been used to analyze and compare with the current version. The detailed improvement designs of double V and inverter delta have been implemented for the high constant torque in a wide range speed of electric motor applications. The torque density, torque ripple, and output power are studied by using the finite element method with different structures. In practice, electromagnetic designs of two-layered rotor structures with types of double V and VI magnets are the best choices because this is a simple structure for manufacturing in mass production. For higher torque density and efficiency, the two-layered double V or VI magnets can adjust the sinusoidal step skewing to minimize harmonic components of the torque ripple and back electromotive force.

Keywords: Interior permanent magnet motor; Finite element method; Double V magnet; Delta-VI magnet and Torque ripple.

1. OVERVIEW

The goal of this paper is to use a vehicle part market model in a long range version marked since 2018. In order to rebuild the geometry construction of the motor model, a tear-down needs to be considered to separate the motor components from the rest of the drive system [1-3].

Figure 1. *Tesla motor model [1].*

The subject motor is produced in the Tesla Model 3 rear-drive unit as shown in figure 1. In many previous papers [2, 3], the given data has shown the single drive system delivers 190-211 kW and 420 – 450 Nm at its peak. This paper focuses on evaluating the characteristics and performance analysis of the electric motor by using the finite element method (FEM) and Motor-CAD software. The obtained results from these techniques will be compared and analyzed to get suitable validation. The study has been carried out independently and the results published here are considered references only.

Figure 2 shows that the motor has been broken to discover the stator and rotor assemblies. It should be noted that the windings are the types of distributed forms. In

this context, the hairpin windings are proposed to replace the distributed forms to improve efficiency.

Figure 2. *Stator assembly.*

For the extended tools, the geometry of the stator is then expressed as the DXF file (with cooling features around the outer perimeter reasonably simplified). Thus, the stator parameters are given in table 1.

Table 1. *Parameters of the stator lamination stack.*

No	Description	Value	Unit
1	Number of stator slots	54	slots
2	Stator lamination outer diameter	225	mm
3	Stator lamination inner diameter	151.3	Mm
4	Lamination stack length	134	Mm
5	Lamination stacking factor	0.95	

The following parameters are measured from the motor with proper instruments given in table 2.

Table 2. *Parameters measured from the motor.*

No	Description	Value	Unit
1	End Winding axial overhang	40	
2	Number of phases	3	Phase
3	Parallel paths	3	
4	Number of turns	2	turn
5	Phase resistance at 20^0C	0.00475	Ohm
6	Number of pole pairs	3	Pole
7	Stator lamination outer diameter	149.9	mm
8	Stator lamination inner diameter	70	mm
9	Magnet dimension	33x21.5x6.5	mm

The rotor assembly and typical rotor lamination of the Tesla model 3 electric motor are presented in figure 3.

The following parameters of the rotor lamination sheet and magnet have been measured. A DXF file then is performed with the later steps. The magnet can be considered in four segments without forming a Halbach array. Both sides of the magnet are measured with the same magnetic field evenly. By using the segmentation of the magnet, the eddy current distribution and self-heating of the magnet themselves will be reduced. The typical rotor lamination produced slots for inserting magnets are presented in figure 3 (*right*). The DXF files obtained from the tear down are then imported into the Motor XP Design Studio. The winding information, and rotor skew information, are manually produced to complete the problem setup. The complete procedure will be presented in the following part of the white paper series. The imported motor cross-section and mesh in Motor XP Design Studio are presented in figure 4.

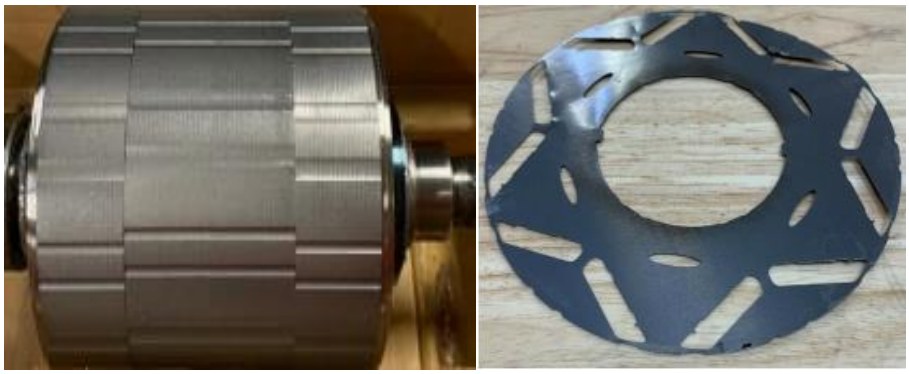

Figure 3. *Rotor assembly (left) and typical rotor lamination (right).*

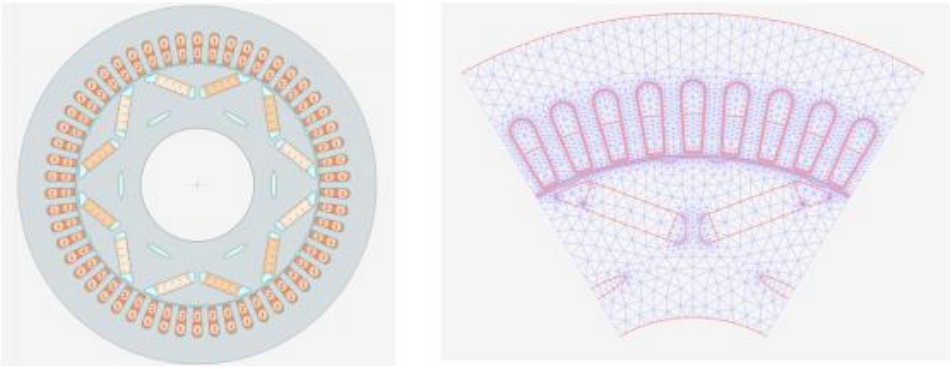

Figure 4. *Imported motor cross-section and mesh in Motor XP Design Studio.*

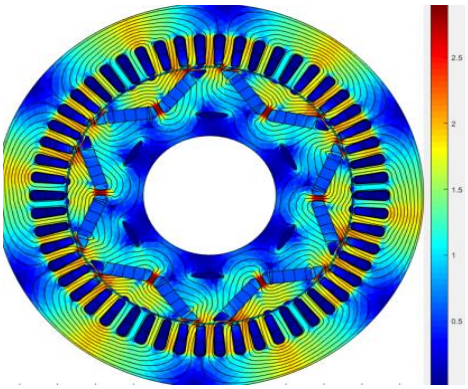

Figure 5. *Flux density distribution in the stator and rotor.*

In practice, the characteristics of the motor can be defined via a magnetostatic analysis for a first principle examination. The torque, voltage, current, loss information and some underlying quantities can be then extracted from this type. The flux density distribution is investigated to show that the motor is not saturated during operation as pointed out in figure 5. It can be seen that the flux density distribution at different parts in the stator and rotor is shown the safety and efficiency of the motor by increasing the torque and current accordingly.

2. ELECTROMAGNETIC DESIGN OF DOUBLE V AND DELTA OF IPM MOTOR

The improvement proposals of IPM motor are designed via an existing IPM with a peak power of 210 kW, torque of 450 Nm, and a maximum speed of 18000 rpm. The main geometry parameters of this motor are given in table 3.

Table 3. *Main geometry parameters of IPM.*

Parameters	**Values**	**Unit**
Slot Number	48	
Stator Lam Dia	225	mm
Stator Bore	150	mm
Tooth Width	4.15	mm
Slot Depth	21.1	mm
Motor Length	150	mm
Stator Lam Length	150	mm
Magnet Length	150	mm
Rotor Lam Length	150	mm
Pole Number	8	
Airgap	0.75	mm

The numbers of slot and poles, stack length, the diameter of stator and rotor, and the air-gap length already given in table 2 are designed for the power inverter of 450VDC/500 A, where the continuous rated power of IPM machine is 190 kW and the maximum speed of the machines is 18000 rpm. The main part of the process is to design the rotor configuration which is an embedded permanent magnet.

An analytical program is developed to compute the flux density distribution and radial force by Matlab coupling to the FEM into one program presented in figure 6. In this program, it is split into several main parts: analytical calculation, exporting drawing, and magnetic stimulation. There are also some supporting parts including the material library which is also associated with the FEM library. A Matlab program coupling to CAD is automatically calculated with the limitations of current and voltage. For the current-limited maximum torque, the electromagnet torque (T_e) can be calculated as [4-6]:

$$T_e = mp\left[\Psi_{1\mathrm{Md}} I \cos\gamma - I^2 \sin\gamma \cos\gamma\left(\mathrm{L_d} - \mathrm{L_q}\right)\right]. \quad (1)$$

Where phase angle γ is the phase angle between the voltage (V_m) and electromotive force (E), L_d is the direct axis inductance, L_q is the quadrature axis inductance, m is the number of phases, p is the number of pole pairs and Ψ_{1Md} is the mutual inductance.

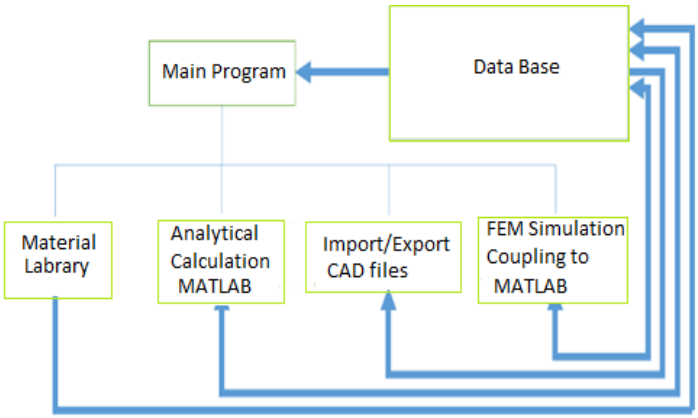

Figure 6. *Analytical program structure.*

For a constant current (I), in order to maximize the torque, the phase angle (γ) is calculated [7-10]

$$\gamma_{Tmax} = sin^{-1}\frac{1}{4}\left[-\frac{\Psi_{1Md}}{\Delta\Psi} + \sqrt{\left(\frac{\Psi_{1Md1}}{\Delta\Psi}\right)^2 + 8}\right] \quad (2)$$

For the constant voltage (V_m), the variable phase angle (δ) between V_m and E, the torque can be calculated by X_d and X_q, that is [10, 11]

$$T_e = \frac{mp}{\omega}\left[\frac{EV_m}{X_d} sin\,\delta + \frac{V_m^2}{2}\left(\frac{1}{X_q} - \frac{1}{X_d}\right) sin\,2\delta\right], \quad (3)$$

Where the terms of X_d and X_q are respectively the direct and quadrature components. In order to find the phase angle (δ) with the maximum torque, it can be computed via:

$$\delta_{Tmax} = \cos^{-1}\left[\left(-\frac{E/V_m}{1-X_d/X_q} \pm \sqrt{\left(\frac{E/V_m}{1-X_d/X_q}\right)^2 + 8}\right)/4\right] \quad (4)$$

The efficiency comparison of the model with double V (2V) and delta (VI) magnets is shown in table 4.

Table 4. *Efficiency comparison of models 2V and VI.*

Parameter	2V	VI	Unit
Average torque	161.63	171.09	Nm
Torque Ripple	17.734	13.19	Nm
Torque Ripple [%]	10.949	7.6935	%
Cogging Torque Ripple (Ce)	2.4068	5.6558	Nm
Input Power	1.72E+05	1.81E+05	Watts
Total Losses (on load)	5767.1	6284.8	Watts
System Efficiency	96.639	96.837	%
Shaft Torque	158.33	167.3	Nm
Armature DC Copper Loss	1951	1951	Watts

(on load)			
Magnet Loss (on load)	14.53	6.006	Watts
Stator iron Loss [total] (on load)	3521	3935	Watts
Rotor iron Loss [total] (on load)	265.6	248.2	Watts
Total Losses (on load)	5767	5685	Watts

In order to check the electromagnetic performances of a 48/8p proposed for IPM motors, the designed model with 2V and VI is considered. The back-electromagnetic forces (EMFs) and torque are computed and analyzed in figures 7 and 8. The obtained results indicate that the VI model has a lower torque ripple and harmonics of back EMF eliminated.

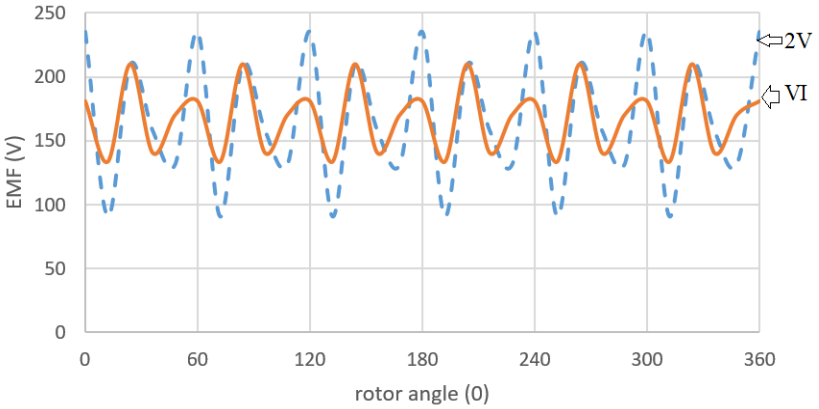

Figure 7. *Back EMF distributions with 2V and VI.*

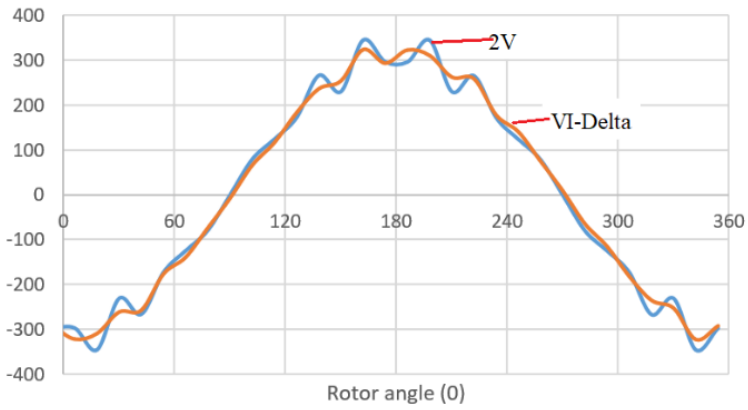

Figure 8. *Torque ripple distribution with 2V and VI.*

3. COGGING TORQUE AND THERMAL ANALYSIS

In order to eliminate the cogging torque by the stator slot-openings, the step-skewing rotor with an angle shift of β mechanical degrees is proposed. Thus, one gets [1-3]:

$$T_{cog} = \sum_{i=0}^{n} T_{ci} \sin(iN(\theta - \beta)) \quad (5)$$

If the rotor is split into several segments along the motor axial direction, and the relative shift angle between the adjacent two rotor poles is β_n mechanical degrees, the resultant cogging torque can be expressed as:

$$T_{cog} = \sum_{i=1}^{n} T_{ci} \sum_{j=0}^{n-1} . \sin(iN(\theta - j\beta_n)) \quad (6)$$

The above equation can be simplified to

$$T_{cog} = \frac{1}{n} \sum_{i=1}^{n} T_{ci} \frac{sin\frac{iN\beta_n n}{2}}{sin\frac{iN\beta_n}{2}} \sin(iN(\theta - j\beta_n)) \quad (7)$$

Hence, for eliminating the *i* order of cogging torque component, the theoretical shift angle β_n must fulfill the following requirements:

$$\sin \frac{iN\beta_n n}{2} = 0 \quad (8)$$

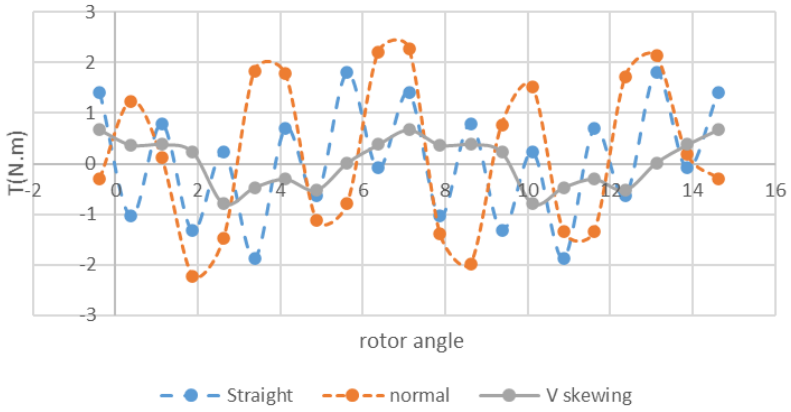

Figure 9. *Cogging torque of six models.*

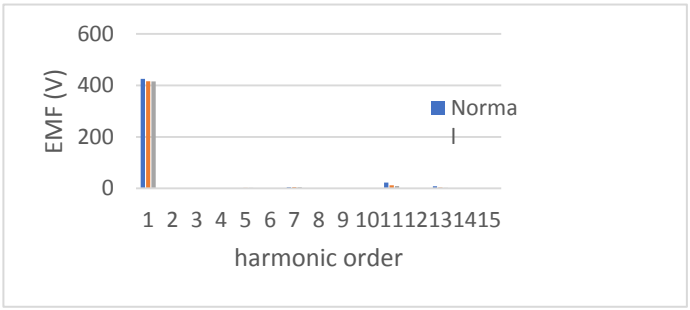

Figure 10. *Back EMF harmonic order analysis of six models.*

By applying the cogging torque for the straight skewing and V- shape skewing magnet model, the conventional skewing model with straight skewing has a smaller shift angle β_n than the V-shape skewing model with the same total skewing angle. The V-shape magnet model has more advantages than the straight skewing because the second harmonic orders can be eliminated together. It can be seen that the harmonic orders with mechanical degrees of 1^0 or 3^0 are reduced to zero if they are fulfilling equation (5). The cogging torque of the three models is also indicated in figure 9. The cogging torque of V-shape skewing design is the lowest value because the double harmonic orders are eliminated in this model. The back EMF harmonics of three models have been analyzed

by the Fourier transform from an EMF waveform with the harmonic order from the first order to the 15th order (figure 10). From the back EMF harmonic results, the total harmonic distortion (TDH) of model 3 with V skewing is the smallest at 4.2%.

The temperature distribution of slot fill and Hairpin windings designs is shown in figure 11. The hot spot of Hairpin winding is 105.7 ^{0}C being lower than 111.5 ^{0}C of the slot fill winding. Based on those results, the IPM motor of V-shape skewing with Hairpin winding design is selected for electric vehicle applications. The efficiency map has been plotted with a speed range of 12000 rpm and a current density of 8.9 A/m2 (figure 12).

The six-segmented magnets prototype is manufactured in figure 13. Each segment with a thickness of 20mm is skewed 1.5 mechanical degrees. To insert six-segment simply, every segment block is designed with one guide pin to fix the correct position when all segments are assembled together.

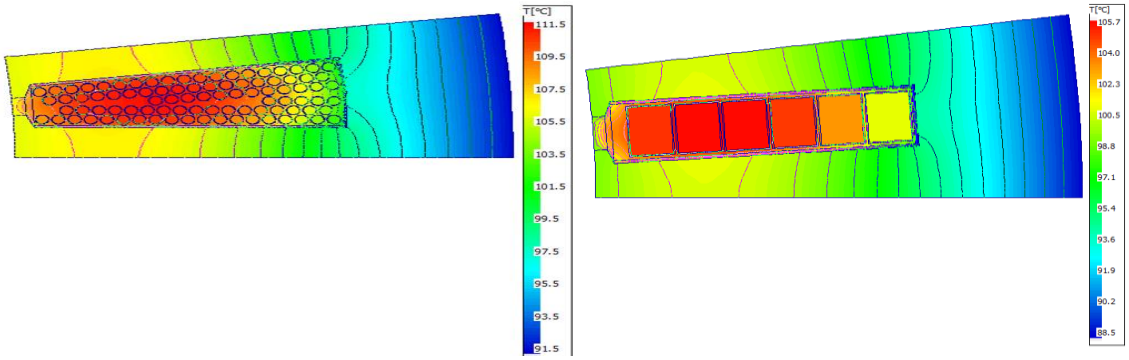

Figure 11. *Temperature distribution of slot fill design (left) and hairpin winding design (right).*

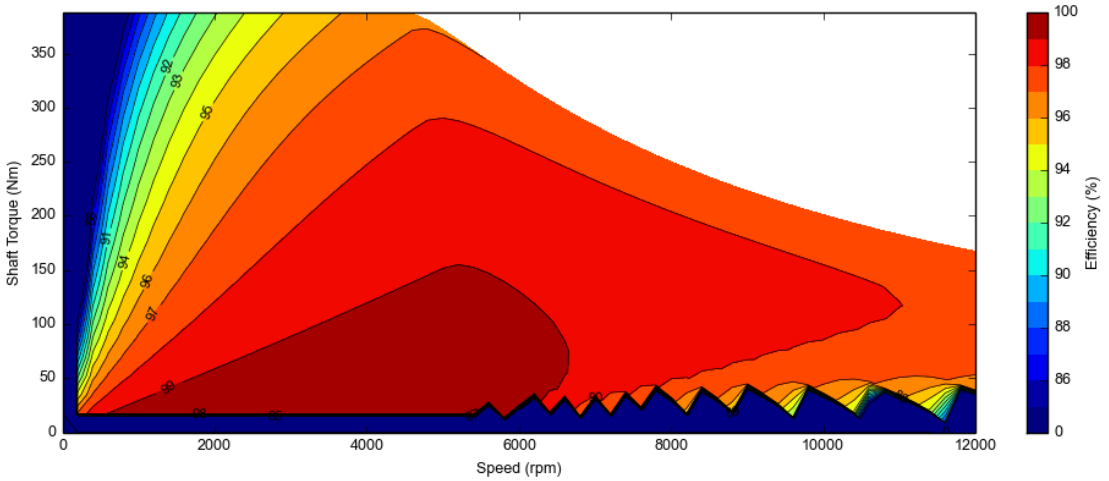

Figure 12. *Efficiency map of hairpin winding design.*

The torque transducer with high accuracy was used to measure torque and speed values under different load conditions. The rotor lamination with six step-V skew magnet slices assembly has been then done production.

Figure 13. *Rotor lamination with six step-V shape skew magnet slices assembly.*

4. CONCLUSIONS

This paper has successfully analyzed and compared the electromagnetic performance of two multi-layered IPM machines for EV applications. The two-layered rotor structure with a VI shape has a better performance. In addition, the model VI design has a lower torque ripple and core loss because the harmonics of air-gap density are reduced by a combination of the I simple and optimal V angle to adjust their performances. The back EMF and torque of the VI model design have been improved from the Tesla model 3 motor.

REFERENCES

[1]. Z. Rezvani, J. Jansson, and J. Bodin, *"Advances in consumer electric vehicle adoption research: A review and research agenda,"* J. Transp. Res. Part D: Transport and Environment, vol. 34, pp. 122-136, Jan. (2015).

[2]. K. T. Chau, C. C. Chan, and C. H. Liu, *"Overview of Permanent-magnet brushless drives for electric and hybrid electric vehicles,"* IEEE Trans. Ind. Electron., vol. 55, no. 6, pp. 2246–2257, Jun. (2008).

[3]. Y. Yang, et al., *"Design and Comparison of Interior Permanent Magn Motor Topologies for Traction Applications,"* IEEE Trans. Transp. Electrification, vol. 3, no. 1, pp. 86–97, Mar. (2017).

[4]. Huynh TA, Hsieh M-F. *"Performance Analysis of Permanent Magnet Motors for Electric Vehicles (EV) Traction Considering Driving Cycles"*. Energies. 11(6):1385, (2018). https://doi.org/10.3390/en11061385

[5]. Liu X, Lin Q, Fu W. *"Optimal Design of Permanent Magnet Arrangement in Synchronous Motors"*. Energies. 10(11):1700, (2017). https://doi.org/10.3390/en10111700

[6]. Çetin, Emrah & Daldaban, Ferhat. *"Analyzing the Profile Effects of the Various Magnet Shapes in Axial Flux PM Motors by Means of 3D-FEA"*. Electronics. 7. 13. 10.3390/electronics7020013, (2018).

[7]. Eklund P, Eriksson S. *"The Influence of Permanent Magnet Material Properties on Generator Rotor Design"*. *Energies*. 12(7):1314, (2019). https://doi.org/10.3390/en12071314

[8]. Lu, C.; Ferrari, S.; Pellegrino, G. *"Two design procedures for PM synchronous machines for electric powertrains"*. IEEE Trans. Transp. Electrif. 3, 98–107, (2017).

[9]. T. A. Huynh, and M.-F. Hsieh, *"Performance analysis of permanent magnet motors for electric vehicles (EV) traction considering driving cycles,"* Energies, vol. 15, no. 8, 2711, May (2018).

[10]. Y. Wang, N. Bianchi, and R. Qu, *"Comparative Study of Non-Rare-Earth and Rare-Earth PM Motors for EV Applications,"* Energies, vol. 9, no. 4, 285, Apr. (2022).

TÓM TẮT

Cải tiến hiệu suất của động cơ IPM thông qua việc thay đổi cấu trúc rotor-ứng dụng cho xe điện

Bài báo nghiên cứu động cơ đồng bộ nam châm vĩnh cửu gắn chìm IPM dẫn động cầu sau của hãng xe điện hãng Tesla với công suất 200 kW- 450 Nm. Nghiên cứu này tập trung vào phân tích và đánh giá hiệu năng của động cơ điện. Các dữ liệu đầu vào và các kết quả mô phỏng cải tiến được sử dụng để phân tích và so sánh so với phiên bản hiện có. Các thiết kế cải tiến mô hình ghép nam châm kiểu kép 2V và kiểu tam giác ngược đã được áp dụng nhằm tạo cho mô-men xoắn duy trì ở mức cực đại ở miền tốc độ rộng được dụng cho xe điện. Mật độ mô-men xoắn, độ gợn mô-men xoắn và công suất đầu ra được nghiên cứu đánh giá dựa trên phương pháp phần tử hữu hạn với các cấu trúc điện từ khác nhau. Trong thực tế, các cấu trúc thiết kế điện từ của kết cấu rôto kiểu kép 2V và VI là sự lựa chọn tốt nhất vì đây là kết cấu đơn giản để chế tạo và sản xuất hàng loạt. Để có mật độ và hiệu suất mô-men xoắn cao hơn, nam châm 2V hoặc VI hai lớp có thể điều chỉnh lệch bước hình sin để giảm thiểu các thành phần hài của đô gợn mô-men xoắn và sức phản điện động.

Từ khoá: Động cơ IPM; Phương pháp phần tử hữu hạn; Cấu trúc nam châm kiểu kép 2V; Cấu trúc nam châm kiểu VI và độ gợn mô men.